RSC Advances

ROYAL SOCIETY OF CHEMISTRY

www.rsc.org/advances

Journal Name

COMMUNICATION

Plasmon Enhanced Fluorescence of Bisphthalonitrile-based Dye via Dopamine Mediated Interfacial Crosslinking Reaction on Silver Nanoparticles

Received 00th January 20xx,
Accepted 00th January 20xx

DOI: 10.1039/x0xx00000x

www.rsc.org/

Kun Jia,*[a,†] Xuefei Zhou,[a,†] Lin Pan,[a] Liting Yuan,[a] Pan Wang,[a] Chunhui Wu,[b] Yumin Huang,[a] and Xiaobo Liu*[a]

A fluorescent dye of phenolphthalein derivative containing bisphthalonitrile groups was synthesized and subsequently chemically grafted onto the dopamine modified silver nanoparticles via the interfacial crosslinking reaction, leading to the enhanced fluorescent emission of dye molecules in solution phase. Specifically, the non-fluorescent phenolphthalein (PP) molecule was end-capped with bisphthalonitrile (BPH) groups through nucleophilic substitution to obtain a violet/blue-emitting fluorescent dye PP-BPH due to the restriction of inter-molecular rotation. Furthermore, the PP-BPH dye can be immobilized on the surface of the dopamine modified silver nanoparticles, given the fact that bisphthalonitrile based monomers can be readily crosslinked in the presence of aromatic amine or phenol compounds (*i.e.* dopamine). Consequently, the fluorescent emission of PP-BPH dye can be further enhanced via the plasmonic enhancement effects of silver nanoparticles. The preliminary results obtained in this communication will pave the way for the plasmon controlled photonic properties of PP-BPH based multifunctional polymers.

Fluorescent spectroscopy is one of the most important techniques widely employed in various fields ranging from bio-imaging, medical diagnostics, (bio)chemical sensing to optoelectronic devices.[1-5] The increased quantum yield or enhanced fluorescent emission of fluorophores is generally required in these fluorescent applications. Given the fact that the fluorescent emission is derived from the electron energy state variation of fluorophores upon receiving photonic excitation, it is believed that manipulation of electromagnetic fields around the fluorophores should be an effective manner to modulate their fluorescent emission.[6] In this context, the plasmonic nanostructures with outstanding capability of intensifying localized electromagnetic field are conjugated with various fluorophores to realize the established technique called plasmon enhanced fluorescence (PEF) that has been widely used in biomedical labelling, molecular sensing, organic electronics, etc.[7-10] The underline principle for the PEF is attributed to the combination of an increase of excitation rate of fluorophores and the increased quantum yield of fluorophores-metal nanostructures system.[11, 12] The efficiency of PEF is dependent on several parameters, including distance between fluorophores and plasmonic nanostructures, structure and morphology of plasmonic nanostructures (composition, size, and shape), fluorescent properties (quantum yield, lifetime) of fluorophores, and spectra overlap between localized surface plasmon resonance (LSPR) band of metal nanostructures and excitation/emission wavelength of fluorophores.[13-16] Among these parameters, the precise control of local distance between fluorophores and plasmonic nanoparticles plays a decisive role in the PEF, as maximized PEF efficiency is only obtained in a critical distance range of 5~10 nm.[17]

The classical PEF experiments have been conducted on a solid substrate patterned with plasmonic nanostructures and dielectric space layer with varying thickness, the emission of fluorophores deposited on this kind of substrate will be obviously enhanced once the metal nanostructure morphology and space layer thickness are optimized.[18] In terms of metal nanostructures, although silver nanoparticles exhibit better optical properties (higher extinction efficient, sharper extinction bands, higher field enhancements) than gold nanoparticles with similar morphology, they have been far less employed in the development of plasmon enhanced spectroscopy or optical sensors, mainly due to the lower chemical stability of silver nanoparticles.[19] With respect to the dielectric space layer, the materials involved in majority of published work are inert silica shell,[20-22] polyelectrolyte multilayers obtained by layer-by-layer (LBL) technique,[23, 24] polymers,[25, 26] or prototypical biomolecules (D-biotin, complementary DNA or streptavidin pairs).[27, 28] Although the local distance between plasmonic nanostructures and fluorophores can be controlled by using these space layers, the attachment of fluorophores on the surface of plasmonic structures is either difficult, time consuming or unstable as fluorophores are basically incorporated with plasmonic nanostructures via non-covalent interaction or physical adsorption methods,[29-31] which would

[a] *Research Branch of Advanced Functional Materials, High Temperature Resistant Polymer and Composites Key Laboratory of Sichuan Province, School of Microelectronics and Solid-State Electronics, University of Electronic Science and Technology of China, Chengdu, 610054, P. R. China. E-mail: jiakun@uestc.edu.cn (Kun Jia), liuxb@uestc.edu.cn (Xiaobo Liu). Tel: +86-28-83207326, Fax: +86-28-83207326.*

[b] *Department of Biophysics, School of Life Science and Technology, University of Electronic Science and Technology of China, Chengdu, 610054, P. R. China.*

† Kun Jia and Xuefei Zhou contribute equally to this work.

Electronic Supplementary Information (ESI) available: [FTIR, ^{1}HNMR spectra of PP-BPH and additional UV-Vis spectra of Ag NPs]. See DOI: 10.1039/x0xx00000x

inevitably limit the practical application of PEF in harsh conditions (*e.g.* high temperature, strong acid medium, etc.) where fluorophores leakage or degradation could be intensified. On the other hand, although the dye fluorescence can be enhanced up to several hundred times under optimized condition, the classical PEF configuration based on solid substrate is still disadvantageous in some practical biosensing or labelling applications, which often are conducted in solution phase.[32]

Therefore, we herein have designed a solution phase active PEF systems on the basis of silver nanoparticles that are surface modified with "active" spacer layer of dopamine (Ag@Dopa NPs). Thanks to the versatile reactivity and exceptional self-adhesive ability of dopamine, the luminescent bisphthalonitrile end-capping phenolphthalein (PP-BPH) dye, a novel precursor for multifunctional hyperbranched phthalocyanines, has been synthesized and further covalently grafted on the Ag@Dopa NPs via the interfacial crosslinking reaction to finally obtain stable nano-emitters of silver-fluorophores with enhanced fluorescence in solution phase.

As shown in **Scheme 1**, the hydroxyl groups of phenolphthalein molecule were successfully substituted with phthalonitrile group of 4-nitrophthalonitrile via a nucleophilic substitution reaction in *N,N*-dimethylformamide (DMF) solvent using potassium carbonate (K_2CO_3) as catalyst, resulting to the fluorescent bisphthalonitrile end-capping phthalonitrile (PP-BPH) dye. On the other hand, silver nanoparticles (Ag NPs) were synthesized via one-pot reduction of silver nitrate ($AgNO_3$) with DMF in the presence of polyvinylpyrrolidone (PVP) as stabilizing agent according to our previous work,[33] afterwards the synthesized Ag NPs were surface coated with poly-dopamine in a base solution and subsequently employed to chemically capture the PP-BPH dye molecules via interfacial crosslinking reaction of bisphthalonitrile monomers (see more details in the experimental section).

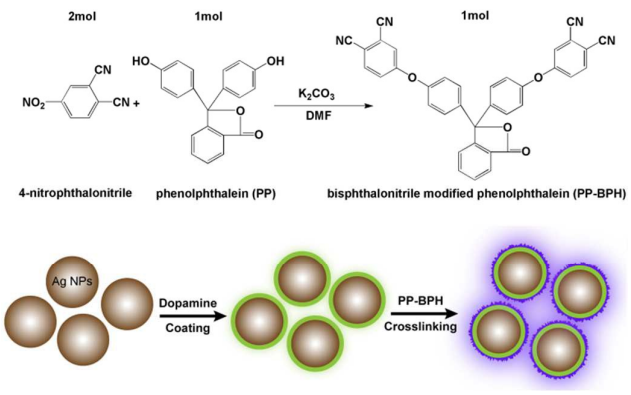

Scheme 1 Chemical route for the synthesis of fluorescent PP-BPH and chemical immobilization on silver nanoparticles modified with dopamine.

Phenolphthalein is widely used as pH indicator in acid-base titrations. Although its molecular structure is only slightly different from that of highly luminescent fluorescein, phenolphthalein is virtually non-fluorescent. The major reason is that the electronically excited states of phenolphthalein are predominately deactivated via the thermal deactivation and in charge separation process, while the fluorescent emission is the dominating process in deactivation of the fluorescein excited states, because the O-bridge in fluorescein leads to a rigid molecular structure, suppressing the energy loss during molecular rotation/oscillation.[34] With this in mind, the end hydroxyl group of phenolphthalein (PP) was substituted with a much larger and more rigid phthalonitrile group in order to obtain a fluorescent phenolphthalein derivative (PP-BPH), which can be employed as photoactive precursor for hyperbranched phthalocyanines synthesis. As shown in **Fig. 1**a, when the same concentration (10^{-5} M) of PP and PP-BPH was solubilized in DMF solvent and excited with 365 nm UV light, the fluorescent emission spectrum of PP-BPH exhibited a strong peak around 420 nm, while the fluorescent emission of PP was rather weak. In addition, the transient fluorescent decay at 420 nm emission of two compounds (excitation at 365 nm) were displayed in **Fig. 1**b, PP-BPH exhibited a much faster fluorescent decay than that of PP, resulting to the fluorescent lifetime decreasing from 3.69 ns for PP to 2.34 ns for PP-BPH, which indicated the radiative decay rate of phenolphthalein was effectively accelerated by the phthalonitrile group substitution. In other words, the electronically excited states of PP-BPH can be deactivated more efficiently via the radiation channel due to its more sterically demanding configuration, thus the fluorescent emission of PP-BPH can be obviously enhanced. The similar fluorescent enhancement mechanism via modification of fluorophore radiative decay rate was well established in plasmon enhanced fluorescence (PEF).[15, 35]

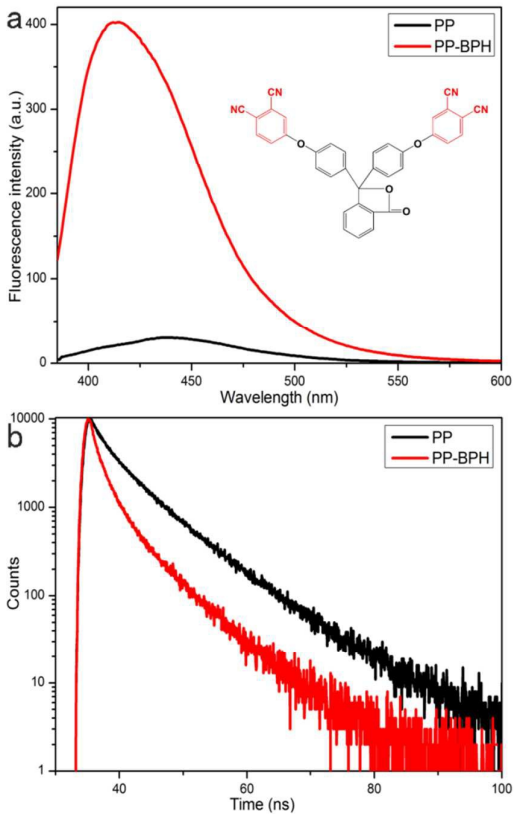

Fig. 1 The steady state fluorescent emission spectra (A) and the transient fluorescent decay (B) of PP and PP-BPH solution in DMF upon excitation at 365 nm, the emission wavelength was 420 nm in fluorescent decay test.

It is well-known that bisphthalonitrile based molecules can be thermally crosslinked by using aromatic amines or phenols compounds as catalyst, and the obtained products are quite thermal stable due to the presence of large amount of aromatic macrocycles structures (isoindoline, triazine, phthalocyanine, etc.).[36, 37] On the other hand, dopamine is widely used as the powerful coating agent for a variety of different materials due to its strong self-adhesive ability, and the coating thickness on materials surface can be readily controlled by the treatment time in the base solution.[38] More importantly, dopamine molecules contain both amine and phenol hydroxyl groups that can effectively trigger the crosslinking reaction of bisphthalonitrile based compounds. Thus, differential scanning calorimetry (DSC) technique was employed to characterize the thermal transition of PP-BPH crosslinking reaction induced by dopamine. As shown in **Fig. 2**, PP-BPH and dopamine exhibit the single strong melting transition at 241 °C and 249 °C with melting enthalpy of 97.11 J/g and 212.4 J/g, respectively. The neat PP-BPH didn't show any exothermal transition, while an obvious exothermic peak located around 295 °C with exothermal enthalpy of 105.3 J/g was detected from the powder mixture of PP-BPH and dopamine, and two independent melting transitions at 238 °C and 246 °C, respectively, were detected from mixture powder. Thus, the DSC thermal analysis confirmed that the dopamine induced crosslinking reaction of PP-BPH.

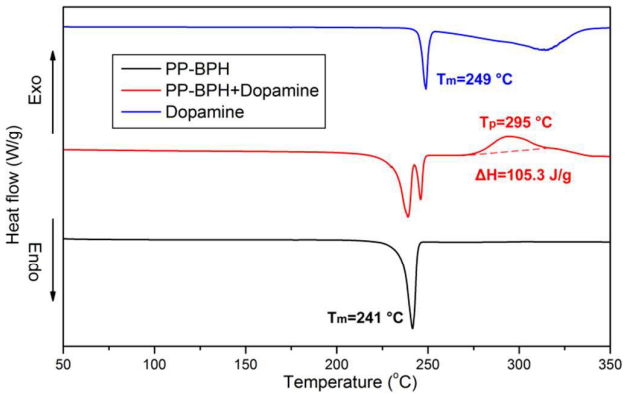

Fig. 2 The DSC curves of PP-BPH, dopamine and PP-BPH/dopamine powder mixtures recoded in nitrogen atmosphere.

Next, the metal nanoparticles were used as an optical near field nanoantenna to further enhance the fluorescence of PP-BPH compound via PEF methodology. In order to maximize the PEF efficiency, the plasmonic band of metal nanostructures should be tuned in the vicinity of excitation or emission wavelength of fluorophore. Given that the emission wavelength of PP-BPH was 420 nm, which was located in the typical range of silver plasmonic bands, thus the silver nanoparticles were synthesized in DMF and further surface modified with dopamine to prevent the potential oxidation, to server as space layer and more importantly, to "capture" the fluorescent PP-BPH molecules. As shown in **Fig. 3**a, the localized surface plasmon resonance (LSPR) wavelength of synthesized Ag NPs was 440 nm, corresponding to the monodispersed 50±10 nm sized silver nanoparticles as displayed in **Fig. 3**b. After the Ag NPs were modified with a dense dopamine layer, an obvious red-shift and broaden of plasmonic peak were recorded, indicating the dopamine was successfully modified on the surface of silver nanoparticles, and the dopamine layer thickness was determined to be around ~10 nm based on the core-shell morphology of Ag@Dopa NPs observed in TEM image in **Fig. 3**c. In addition, it should be noted that the obtained Ag@Dopa NPs are quite stable both in water and DMF solvent, as their LSPR spectrum remained unchanged for at least 1 month when stored at room temperature. The solution stability of Ag@Dopa NPs was mainly attributed to the presence of dense and robust poly-dopamine layer on the surface of Ag NPs, effectively preventing the potential oxidation and solution-driven ripening process of silver nanoparticles. Therefore, the obtained Ag@Dopa NPs with good stability and reproducible optical properties can be employed as the robust and reactive near-field nanoantenna to covalently immobilize fluorescent dyes.

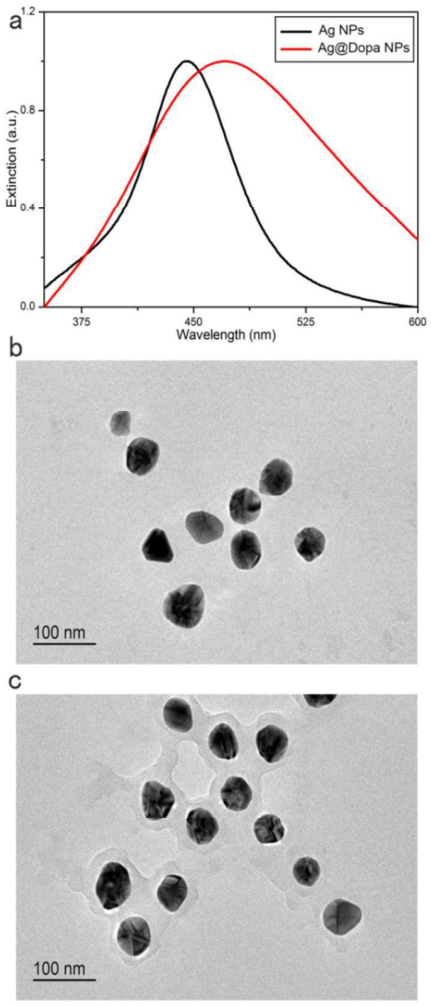

Fig. 3 The extinction spectra (a) and transmission electron microscope (TEM) images of Ag NPs (b) and dopamine modified Ag NPs (c).

Furthermore, the Ag@Dopa NPs were dispersed in DMF solution containing 0.01 M PP-BPH, followed by heating at refluxing to capture the fluorophores via the interfacial crosslinking between dopamine and PP-BPH. After reaction for different time, PP-BPH was immobilized on the surface of Ag@Dopa NPs, which was confirmed by the steady red-shift of their LSPR bands as well (see **Fig. S1** in Electronic Supplementary Information, ESI). Next, the nano-conjugates of Ag@Dopa@PP-BPH were separated via centrifugation, purified and then re-dispersed in DMF solvent for fluorescent spectroscopy measurement. In order to determine the effects of active polydopamine layer, the control experiments were conducted following the same protocol except that the as-synthesized Ag NPs were used. It was clear from **Fig. 4**a that the steady state fluorescent intensities of PP-BPH compounds crosslinked on the Ag@Dopa NPs were generally larger than those of PP-BPH physically adsorbed on Ag NPs without dopamine coatings. More specifically, the fluorescent emission was gradually intensified from Ag@Dopa@PP-BPH NPs as the increasing of reaction time, while the fluorescence of Ag@PP-BPH NPs was slightly decreased after a longer time reaction. In another control experiment, the unmodified Ag NPs or Ag@Dopa NPs were directly admixed with PP-BPH solution for fluorescent measurement, respectively, it was found that the PP-BPH fluorescence was strongly quenched by the unmodified Ag NPs, but was nearly unchanged in the presence of Ag@Dopa NPs (see **Fig. S2** in ESI). Moreover, the transient fluorescent decay of Ag@PP-BPH and Ag@Dopa@PP-BPH for reaction time of 2 h was displayed in **Fig. 4b**, where the faster fluorescent decay and corresponding reduced lifetime was observed from the nano-conjugates containing active dopamine layer. The reduced lifetime in this case implied that the fluorescent decay rate of PP-BPH fluorophores was enhanced, which resulted to the improved photostability, quantum yields and emission intensity of fluorophores located in the vicinity of Ag@Dopa NPs nanoantenna. In addition, the fluorescent lifetime of various compounds and fluorescent nano-conjugates were summarized in **Table 1**. All these experimental results demonstrated that dopamine is indispensable in the Ag NPs enhanced fluorescence of PP-BPH.

Table 1. Fluorescent lifetime of various compounds and nano-conjugates involved in this work.

Sample / Lifetime (ns)	PP	PP-BPH	Ag@PP-BPH_120min	Ag@Dopa@PP-BPH_120min
Decay 1	4.11	2.74	3.11	1.22
Decay 2	9.16	1.27	7.76	8.95
Lifetime	3.69	2.34	2.59	1.84

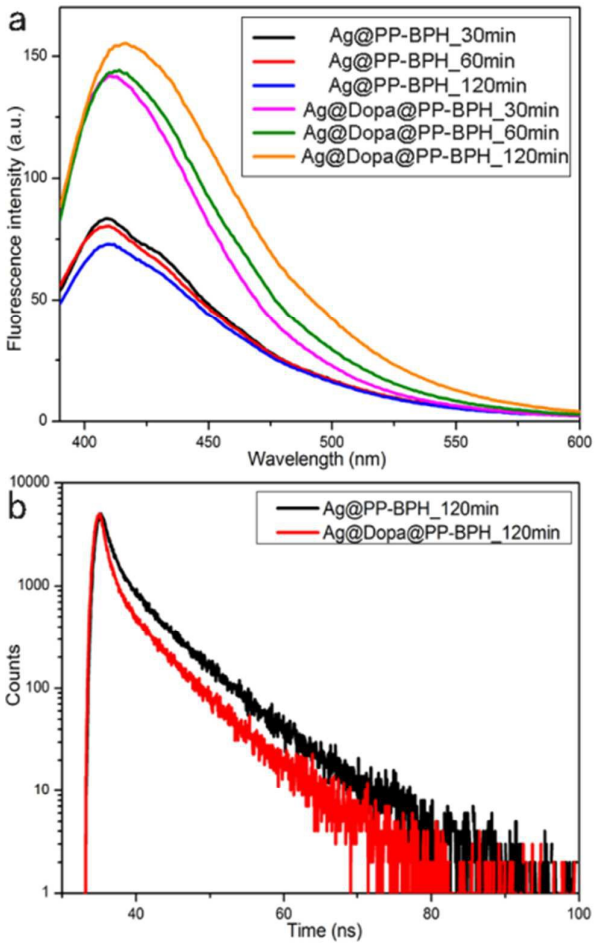

Fig. 4 The steady fluorescent emission spectra (a) and transient fluorescent decay of various nano-conjugates synthesized for different reaction time.

Conclusions

In summary, the fluorescent phenolphthalein derivative end-capped with bisphthalonitrile groups were synthesized and subsequently chemically immobilized on the surface of dopamine coated silver nanoparticles via the crosslinking reaction. To our best knowledge, this is the first report of plasmon enhanced fluorescence (PEF) in organic solution phase using dopamine as active space layer to chemically position the bisphthalonitrile based fluorophores on the surface of plasmonic nanostructures. Although the fluorescent enhancement factor is still low for the moment, it will be obviously increased after the optimization of plasmonic nanostructures morphology and dopamine layer thickness. On the other hand, bisphthalonitrile is an important kind of precursors for the synthesis of hyperbranched phthalocyanines, which are considered as the versatile building blocks for design of multifunctional composites, besides the as-synthesized and crosslinked form of PP-BPH are both luminescent according to our experimental results, therefore the advanced nanohybrids with enhanced photonic

properties would be constructed through the dopamine mediated crosslinking reaction of fluorescent bisphthalonitrile compounds on the surface of plasmonic nanostructures. These works are currently in progress in our lab.

Experimental Section

Synthesis of PP-BPH. Phenolphthalein (38.16 g, 0.12 mol), 4-nitrophthalonirile (34.6 g, 0.2 mol), K_2CO_3 (36.43 g, 0.26 mol) were added into a three-necked flask where contains 50 mL DMF solvent, then the mixture was heated at 60 °C in a water bath for 8 h. Afterwards, the reaction products were precipitated in dilute hydrochloric acid solution, followed by washing with hot ddH_2O, ethanol and purified with silica gel column. The chemical structure of purified compound was characterized with FTIR (-CN: 2232 cm^{-1}, -C=O: 1761 cm^{-1}, -O-: 1248 cm^{-1}, **Fig. S3** in ESI) and ^{1}H NMR (DMSO-d_6, 400 MHz): δ= 7.23 (d, J= 8 Hz, 4H), 7.43-7.48 (m, 6H), 7.72 (t, J= 7.6 Hz, 1H), 7.86-7.92 (m, 3H), 7.97 (d, J= 8.4 Hz, 2H), 8.10(d, J= 8.8 Hz, 2H) ppm. ^{13}C NMR (DMSO-d_6, 100 MHz): δ= 90.1, 108.7, 115.3, 115.8, 116.8, 120.3, 122.6, 123.2, 124.3, 124.6, 125.7, 129.1, 130.2, 135.3, 136.3, 137.5, 151.2, 154.2, 160.4, 168.6 ppm. MS (ESI^+): calcd for $C_{36}H_{18}N_4O_4Na$ $[M+Na]^+$ 593.12, found 593.12. Anal. Calcd for $C_{36}H_{18}N_4O_4 \cdot H_2O$ (%): C, 73.46; H, 3.43; N, 9.52, found: C, 73.16; H, 3.05; N, 9.07.

Synthesis of Ag NPs and surface coating with dopamine. Monodispersed silver nanospheres were synthesized according to the protocol used in our previous work with slight modification. Then, the purified Ag NPs (0.25 nM) were incubated in a base solution (pH=8.5) containing 10 mM dopamine for 2h at room temperature, followed by centrifugation (8000 rpm, 5 min) and washing with fresh DMF for two times, finally the dopamine coated Ag NPs were stored in DMF solution at 4 °C for further experiment.

Preparation of Ag@Dopa@PP-BPH fluorescent nano-conjugates. The previously synthesized PP-BPH (1.2 g) was solubilized with 8 mL DMF solvent in a flask equipped with condenser and magnetic stirrer, followed by addition of 2 mL DMF solution containing Ag@Dopa NPs. Next, the reaction mixture were heated to reflux for different time (0.5 h, 1h and 2h), and then the solution was freely cooled down and the fluorescent Ag@Dopa@PP-BPH nano-conjugates were obtained by centrifugation (8000 rpm, 5 min) and washing with fresh DMF twice. In the control experiments, the as-synthesized Ag NPs without dopamine coating layer were reacted directly with PP-BPH and purified following the same protocol.

Characterization methods. The Fourier transform infrared (FTIR) spectra were recorded using a Shimadzu 8400S FTIR spectrometer. NMR spectra were obtained with a Bruker AV II-400 spectrometer. The ^{1}H NMR (400 MHz) chemical shifts and the ^{13}C NMR (100 MHz) chemical shifts were measured relative to DMSO-d_6 (H: δ = 2.50 ppm; C: δ = 39.52 ppm) as the internal references. Low-resolution mass spectra (MS) were obtained by ESI-MS. Elemental analysis data were obtained on EA FLASH 1112 SERIES. The thermal transition analysis was conducted in a differential scanning calorimetry (DSC, TA, Q100) under nitrogen atmosphere (50 mL/min) using the heating rate of 10 °C/min. The morphology of synthesised Ag NPs and Ag@Dopa NPs was characterized with transmission electron microscope (TEM, JEOL, JEM-2100F operating at 200.0 kV). The size distribution and dopamine layer thickness of obtained silver nanoparticles were analysed by the public domain software of ImageJ developed by National Institutes of Health. The localized surface plasmon resonance (LSPR) spectra and fluorescent excitation/emission spectra were recorded using a Persee TU 1901 UV-Vis spectrophotometer and a fluorescence spectrophotometer (F-4600, Hitachi), respectively. The time-correlated photoluminescent decay and fluorescent lifetime were determined by using Horiba Jobin Yvon Tempro-01 instrument.

Acknowledgements

The authors gratefully thank the financial support from National Natural Science Foundation of China (Project No. 51373028, No. 51403029), "863"National Major Program of High Technology (2012AA03A212), South Wisdom Valley Innovative Research Team Program and Ningbo Major (key) Science and Technology Research Plan (2013B06011).

Notes and references

1. K. P. Carter, A. M. Young and A. E. Palmer, *Chem. Rev.*, 2014, **114**, 4564-4601.
2. H. N. Kim, W. X. Ren, J. S. Kim and J. Yoon, *Chem. Soc. Rev.*, 2012, **41**, 3210-3244.
3. A. M. Pekkanen, M. R. DeWitt and M. N. Rylander, *J. Biomed. Nanotechnol.*, 2014, **10**, 1677-1712.
4. X. Yang, G. Zhou and W.-Y. Wong, *J. Mater. Chem. C*, 2014, **2**, 1760-1778.
5. Z. Ahmed and K. Iftikhar, *RSC Advances*, 2014, **4**, 63696-63711.
6. K. A. Kang and J. Wang, *J. Nanobiotechnol.*, 2014, **12**, 56.
7. J. Peng, X. Xu, Y. Tian, J. Wang, F. Tang and L. Li, *Appl. Phys. Lett.*, 2014, **105**, 173301.
8. H. Chen and Y. Xia, *Anal. Chem.*, 2014, **86**, 11062-11069.
9. K. Aslan, I. Gryczynski, J. Malicka, E. Matveeva, J. R. Lakowicz and C. D. Geddes, *Curr. Opin. Biotechnol.*, 2005, **16**, 55-62.
10. Y. K. Xu, S. Hwang, S. Kim and J. Y. Chen, *ACS Appl. Mater. Interfaces*, 2014, **6**, 5619-5628.
11. F. Tam, G. P. Goodrich, B. R. Johnson and N. J. Halas, *Nano Lett.*, 2007, **7**, 496-501.
12. K. Aslan, Z. Leonenko, J. R. Lakowicz and C. D. Geddes, *J. Fluoresc.*, 2005, **15**, 643-654.
13. T. Ming, H. Chen, R. Jiang, Q. Li and J. Wang, *J. Phys. Chem. Lett.*, 2011, **3**, 191-202.
14. R. Bardhan, N. K. Grady, J. R. Cole, A. Joshi and N. J. Halas, *ACS Nano*, 2009, **3**, 744-752.
15. N. S. Abadeer, M. R. Brennan, W. L. Wilson and C. J. Murphy, *ACS Nano*, 2014, **8**, 8392-8406.
16. Y. Zhang, A. Dragan and C. D. Geddes, *J. Phys. Chem. C*, 2009, **113**, 12095-12100.

17. W. Hong, Y. Zhang, L. Gan, X. Chen and M. Zhang, *J. Mater. Chem. C*, 2015, **3**, 6185-6191.
18. S.-Y. Liu, L. Huang, J.-F. Li, C. Wang, Q. Li, H.-X. Xu, H.-L. Guo, Z.-M. Meng, Z. Shi and Z.-Y. Li, *J. Phys. Chem. C*, 2013, **117**, 10636-10642.
19. C. Wang, Y. Kuang, L. Luo and X. Sun, *J. Mater. Chem. C*, 2013, **1**, 4146-4152.
20. N. M. Kha, C.-H. Chen, W.-N. Su, J. Rick and B.-J. Hwang, *Phys. Chem. Chem. Phys.*, 2015, DOI: 10.1039/C4CP05217J.
21. Y. Liu, C.-y. Liu, Z.-y. Zhang, W.-d. Yang and S.-d. Nie, *J. Mater. Chem. C*, 2015, **3**, 2881-2885.
22. C. D. Geddes, H. Cao, I. Gryczynski, Z. Gryczynski, J. Fang and J. R. Lakowicz, *J. Phys. Chem. A*, 2003, **107**, 3443-3449.
23. N. Gandra, C. Portz, L. Tian, R. Tang, B. Xu, S. Achilefu and S. Singamaneni, *Angew. Chem., Int. Ed.*, 2014, **53**, 866-870.
24. A. V. Sorokin, A. A. Zabolotskii, N. V. Pereverzev, I. I. Bespalova, S. L. Yefimova, Y. V. Malyukin and A. I. Plekhanov, *J. Phys. Chem. C*, 2015, **119**, 2743-2751.
25. J. Chen, Y. Jin, N. Fahruddin and J. X. Zhao, *Langmuir*, 2013, **29**, 1584-1591.
26. R. Das, P. Phadke, N. Khichar and S. Chawla, *J. Mater. Chem. C*, 2014, **2**, 8880-8885.
27. B. Abel, S. Coskun, M. Mohammed, R. Williams, H. E. Unalan and K. Aslan, *J. Phys. Chem. C*, 2015, **119**, 675-684.
28. K. Aslan, J. Lakowicz, H. Szmacinski and C. Geddes, *J. Fluoresc.*, 2004, **14**, 677-679.
29. S. Rangełowa-Jankowska, D. Jankowski, B. Grobelna, I. Gryczyński, Z. Gryczyński, R. Bogdanowicz and P. Bojarski, *Chemphyschem*, 2011, **12**, 2449-2452.
30. R. Zhang, Z. Wang, C. Song, J. Yang, J. Li, A. Sadaf and Y. Cui, *Chemphyschem*, 2011, **12**, 992-998.
31. K. Aslan, M. Wu, J. R. Lakowicz and C. D. Geddes, *J. Am. Chem. Soc.*, 2007, **129**, 1524-1525.
32. R. Li, S. Xu, C. Wang, H. Shao, Q. Xu and Y. Cui, *Chemphyschem*, 2010, **11**, 2582-2588.
33. K. Jia, P. Wang, L. Yuan, X. Zhou, W. Chen and X. Liu, *J. Mater. Chem. C*, 2015, **3**, 3522-3529.
34. A. Boguta and D. Wróbel, *J. Fluoresc.*, 2001, **11**, 129-137.
35. E. Heydari, I. Pastoriza-Santos, R. Flehr, L. M. Liz-Marzán and J. Stumpe, *J. Phys. Chem. C*, 2013, **117**, 16577-16583.
36. D. D. Dominguez and T. M. Keller, *Polymer*, 2007, **48**, 91-97.
37. K. Jia, R. Zhao, J. Zhong and X. Liu, *J. Mater. Sci: Mater. Electron.*, 2010, **21**, 1125-1131.
38. K. Jia, M. Y. Khaywah, Y. Li, J. L. Bijeon, P. M. Adam, R. Déturche, B. Guelorget, M. François, G. Louarn and R. E. Ionescu, *ACS Appl. Mater. Interfaces*, 2014, **6**, 219-227.